



## Polymerization of Norbornene

## Switchable Polymerization of Norbornene Derivatives by a Ferrocene-Palladium(II) Heteroscorpionate Complex

Mark Abubekero<sup>[a]</sup> Scott M. Shepard<sup>[a]</sup> and Paula L. Diaconescu<sup>\*[a]</sup>

**Abstract:** The ferrocene-chelating heteroscorpionate complex  $[(\text{fc}(\text{PPh}_2)\{\text{BH}(\{3,5\text{-Me}_2\text{pz}\}_2)\})\text{PdMe}] \{(\text{fc}^{\text{P}^{\text{B}}})\text{PdMe}$ ,  $\text{fc} = 1,1'$ -ferrocenediyl,  $\text{pz} = \text{pyrazole}\}$  catalyzes the addition polymerization of norbornene and norbornene derivatives upon oxidation with  $[\text{AcFc}][\text{BAR}^{\text{F}}]$  {acetyl ferrocenium tetrakis(3,5-bis(trifluoromethyl)-

phenyl)borate}. In situ reduction of  $[(\text{fc}^{\text{P}^{\text{B}}})\text{PdMe}][\text{BAR}^{\text{F}}]$  in the presence of a substituted norbornene results in significant decrease of catalytic activity. Addition of one equivalent of oxidant restores the activity.

## Introduction

Vinyl polynorbornenes are important materials for optical applications due to their excellent thermal stability, high glass transition temperatures, small birefringence, and dielectric loss.<sup>[1–5]</sup> However, polynorbornenes are brittle, even at high molecular weights, display poor adhesion to common substrates, poor solubility in common organic solvents, and cannot be melt processed due to decomposition.<sup>[6–9]</sup> Modifying the norbornene monomers with functional groups increases the solubility of the resulting polymers and improves their processability.<sup>[10]</sup> The substitution of norbornenes, typically at the 5-position, can be achieved via a Diels–Alder reaction, in some cases, directly from dicyclopentadiene and a dienophile.<sup>[11]</sup> Polymers obtained from the substituted monomers show improved adhesive and mechanical properties while retaining similar optical properties as the unsubstituted polynorbornenes.<sup>[1,4,12]</sup>

Amongst transition metal catalysts, palladium-based systems are highly active toward norbornene polymerization and produce high molecular weight vinyl polynorbornenes.<sup>[1,13–20]</sup> Most palladium catalysts feature bidentate or monodentate supporting ligands since an open coordination sphere is necessary for monomer coordination.<sup>[9,10,13–15,21–25]</sup> Commonly employed systems also require the use of strong Lewis acids/alkylating reagents (i.e. methylalumoxane, fluorinated arylboranes/alkylaluminum complexes) as co-catalysts to generate a metal-alkyl fragment and an empty coordination site.<sup>[1,26]</sup> The resulting catalytic species are typically not stable in the absence of monomer, and in certain cases, have further complications arising from the possible monomer/co-catalyst interactions.<sup>[15,27]</sup> Alternatively, in cases when an open coordination sphere cannot be readily obtained, such as allyl palladium complexes, the use of

hemilabile supporting ligands has been reported.<sup>[28]</sup> Weakly coordinating components of these ligands can be readily displaced by more nucleophilic olefins. On the other hand, the use of a tridentate supporting ligand would severely limit the availability of an empty coordination site. A possible solution is the incorporation of a labile component into the ligand framework, similar to those in hemilabile ligands, resulting in an effective polymerization system without the need for a co-catalyst. Additionally, controlling the lability of a supporting ligand can be accomplished by a method similar to the one utilized in redox-switchable hemilabile ligands.<sup>[29]</sup> An appropriate placement of a redox-active group into a ligand framework provides a method of influencing both the electronic and steric properties of the transition metal complex through oxidation of the ligand. Because of our interest in redox active ferrocene-based chelating ligands,<sup>[30–34]</sup> we set out to investigate the effects of the redox switch on the lability of the ferrocene-chelating heteroscorpionate ligand in the methylpalladium complex,  $[(\text{fc}(\text{PPh}_2)\{\text{BH}(\{3,5\text{-Me}_2\text{pz}\}_2)\})\text{PdMe}] \{(\text{fc}^{\text{P}^{\text{B}}})\text{PdMe}$ ,  $\text{fc} = 1,1'$ -ferrocenediyl,  $\text{pz} = \text{pyrazole}\}$ , in the presence of norbornene derivatives. Herein, we report the first palladium system supported by a tridentate ligand modified by an on/off redox switch for the addition polymerization of norbornene and norbornene derivatives.

## Results and Discussion

## Synthesis and Characterization of Palladium Complexes

The palladium complex (COD)PdMeCl was prepared via transmetallation of (COD)PdCl<sub>2</sub> with trimethylaluminum, instead of using alkyl tin reagents,<sup>[35]</sup> in a mixture of THF and diethyl ether, similarly to the synthesis of  $[\text{Pd}_2(\mu\text{-Cl})_2\text{Me}_2(\text{PET}_3)_2]$ .<sup>[35]</sup> The characterization of the desired product was accomplished by <sup>1</sup>H NMR spectroscopy (Figure S1), which was consistent with previously published results.<sup>[36]</sup>

Addition of  $(\text{fc}^{\text{P}^{\text{B}}})\text{Li}(\text{THF})_2$  to (COD)PdMeCl in THF led to the isolation of  $(\text{fc}^{\text{P}^{\text{B}}})\text{PdMe}\cdot(\text{C}_7\text{H}_8)$  as red crystals in 77.1 % yield; see

[a] Department of Chemistry and Biochemistry, University of California, Los Angeles, 607 Charles E. Young Drive East, Los Angeles, CA 90095, USA  
E-mail: pld@chem.ucla.edu  
<http://copper.chem.ucla.edu/pldgroup/index.htm>

Supporting information for this article is available on the WWW under <http://dx.doi.org/10.1002/ejic.201501295>.

Equation (1). The solid-state molecular structure of  $(\text{fc}^{\text{P}^{\text{B}}})\text{PdMe}$  was determined using single-crystal X-ray diffraction (Figure 1). The coordination environment around the palladium center is in a distorted square-planar geometry ( $\tau = 0.16$ )<sup>[37]</sup> similar to the nickel analogue,  $(\text{fc}^{\text{P}^{\text{B}}})\text{NiMe}$ .<sup>[38]</sup> The metal-donor atom distances [P(1)–Pd(1), 2.2107(4) Å; C(1)–Pd(1), 2.0454(18) Å; N(3)–Pd(1), 2.0938(14) Å; N(1)–Pd(1), 2.1097(14) Å] are comparable with values reported for similar complexes: 1-(mesityl)-3-(2-hydroxyphenyl)-4,5-dihydro-imidazolyl methyl triphenylphosphine palladium(II) [Pd–P, 2.2858(9) Å; Pd–C, 2.041(3) Å],<sup>[39]</sup>  $(\text{Tp}^{\text{Me,Me}})\text{Pd}(\text{methallyl})$  [ $\text{Tp}^{\text{Me,Me}} = \text{hydrotris}(3,5\text{-dimethylpyrazolyl})\text{borate}$ , Pd–N, 2.090(2) and 2.086(2) Å].<sup>[40]</sup> However, unlike for the nickel analogue, the resonance signals in the corresponding  $^1\text{H}$  NMR spectrum (Figure S2) are sharp, easily discernible, and are consistent with a diamagnetic complex.

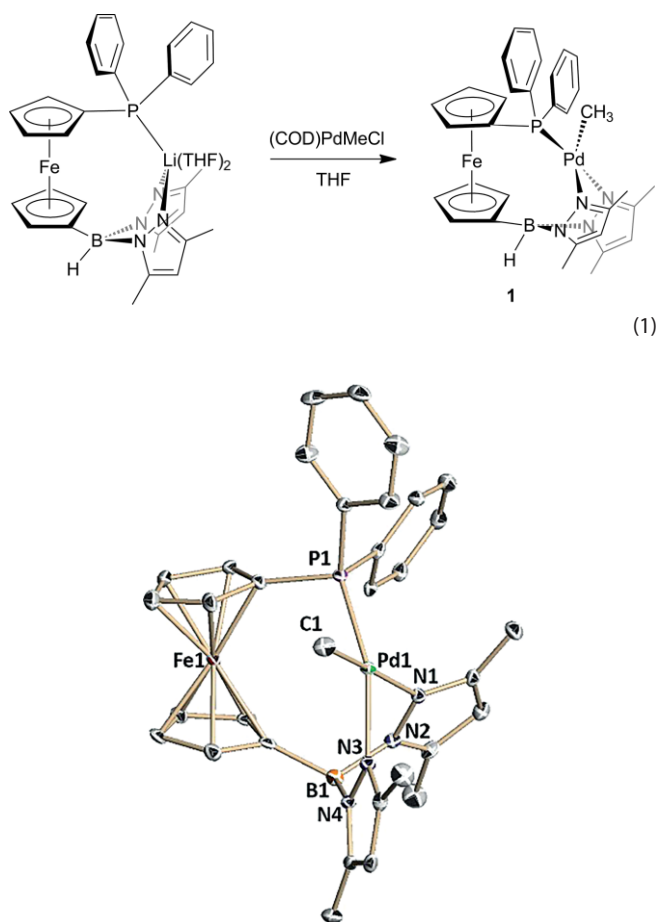


Figure 1. Molecular structure drawing of  $(\text{fc}^{\text{P}^{\text{B}}})\text{PdMe}$  with thermal ellipsoids at 50 % probability; hydrogen atoms are omitted for clarity. Selected distances [Å] and angles [°]: P(1)–Pd(1), 2.2107(4); C(1)–Pd(1), 2.0454(18); N(1)–Pd(1), 2.1097(14); N(3)–Pd(1), 2.0938(14); P(1)–Pd(1)–C(1), 88.41(5); C(1)–Pd(1)–N(3) 91.71(7); P(1)–Pd(1)–N(1), 95.98(4); N(1)–Pd(1)–N(3), 84.99(5); C(1)–Pd(1)–N(1), 174.78(6); C(1)–Pd(1)–P(1), N(3)–Pd(1)–P(1), 161.95(4).

Electrochemical studies performed on  $(\text{fc}^{\text{P}^{\text{B}}})\text{PdMe}$  show a quasi-reversible curve with a redox potential of  $-0.27$  V vs.  $\text{Fc}/\text{Fc}^+$  (Figure 2), suggesting that ferrocenium salts may be used as chemical oxidants. On an NMR scale, the oxidation of the palladium complex with one equivalent of acetyl ferrocenium

tetrakis[3,5-bis(trifluoromethyl)phenyl]borate ( $[\text{AcFc}][\text{BAR}^{\text{F}}]$ ) results in the appearance of paramagnetically shifted and broadened signals in the  $^1\text{H}$  NMR spectrum (Figure S8). The  $^{11}\text{B}$  NMR spectrum (Figure S10) shows a significant upfield shift of the signal corresponding to the  $(\text{fc}^{\text{P}^{\text{B}}})\text{PdMe}$  complex, from  $-7.6$  to  $-65.2$  ppm, upon oxidation. However, the oxidized complex is  $^{31}\text{P}$  NMR silent. Reduction with one equivalent of cobaltocene ( $\text{Cp}_2\text{Co}$ ) restores the original complex,  $(\text{fc}^{\text{P}^{\text{B}}})\text{PdMe}$ , with no appearance of decomposition or side products (Figures S6 and S7). On a larger scale, the addition of  $(\text{fc}^{\text{P}^{\text{B}}})\text{PdMe}$  to a suspension of  $[\text{AcFc}][\text{BAR}^{\text{F}}]$  in toluene resulted in the isolation of  $[(\text{fc}^{\text{P}^{\text{B}}})\text{PdMe}][\text{BAR}^{\text{F}}]$  as dark brown solids in 84 % yield; see Equation (2). The presence of the  $[\text{BAR}^{\text{F}}]$  counterion was confirmed by the presence of a singlet at  $\delta = -6.1$  and  $-62.2$  ppm in the  $^{11}\text{B}$  and  $^{19}\text{F}$  NMR spectra (Figures S10 and S9), respectively. Attempts to grow X-ray quality crystals from various neat solvents and solvent combinations were unsuccessful and only dark brown oils were obtained. However, besides spectroscopic characterization, elemental analysis also agrees with the formulation of  $[(\text{fc}^{\text{P}^{\text{B}}})\text{PdMe}][\text{BAR}^{\text{F}}]$ .

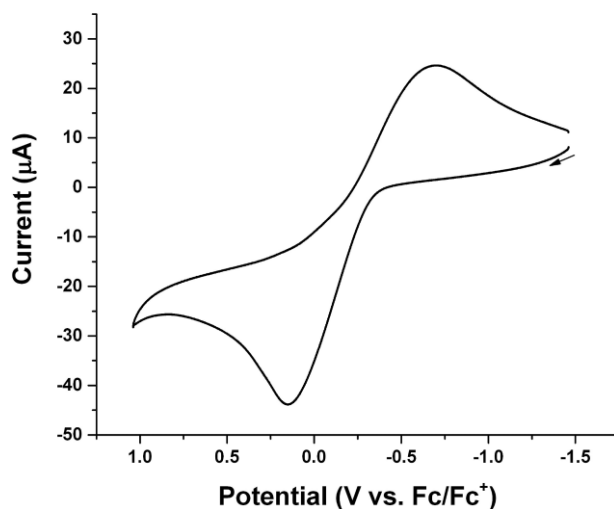


Figure 2. Cyclic voltammogram recorded with a glassy carbon electrode at 100 mV/s in THF, 0.10 M  $[\text{nBu}_4\text{N}][\text{PF}_6]$  containing 5.0 mM  $(\text{fc}^{\text{P}^{\text{B}}})\text{PdMe}$ .

Knowing the strength of the palladium–phosphorus and palladium–nitrogen bonds in  $(\text{fc}^{\text{P}^{\text{B}}})\text{PdMe}$  is necessary for understanding its catalytic activity. Addition of four equivalents of *tert*-butyl isocyanide (*t*BuNC) to  $(\text{fc}^{\text{P}^{\text{B}}})\text{PdMe}$  resulted in the isolation of  $(\text{fc}^{\text{P}^{\text{B}}})\text{Pd}[\text{C}(\text{Me})\text{N}t\text{Bu}](\text{CN}t\text{Bu})\cdot(\text{C}_7\text{H}_8)$  as an orange crystalline material; see Equation (3). The new compound is the product of a migratory insertion of one equivalent of *t*BuNC into the palladium–carbon bond and the coordination of a second equivalent of *t*BuNC to the palladium metal center.<sup>[41,42]</sup> The two pyrazoles are not chemically equivalent in the  $^1\text{H}$  NMR spectrum (Figure 3), suggesting that only one of them is coordinated to palladium. The phosphine is in a solution state equilibrium between a free and palladium bound phosphine as observed by two peaks at  $-14.9$  and  $9.4$  ppm, respectively, in the  $^{31}\text{P}$  NMR spectrum (Figure S15).<sup>[43]</sup> However, no reaction occurs

upon the addition of benzonitrile or ferrocenyldiphenylphosphine to  $(\text{fc}^{\text{PB}})\text{PdMe}$ , suggesting that weaker nucleophiles cannot displace the supporting ligand. Similarly, addition of acetonitrile to  $[(\text{fc}^{\text{PB}})\text{PdMe}][\text{BAR}^{\text{F}}]$  results in no reaction. However, oxidation  $(\text{fc}^{\text{PB}})\text{PdMe}$  with  $[\text{AcFc}][\text{BAR}^{\text{F}}]$  in the presence of ferrocenyldiphenylphosphine results in the disappearance of the two  $^{31}\text{P}$  NMR singlets at  $\delta = 30.5$  and  $-16.1$  ppm (Figure S11) that correspond to the two ferrocene compounds, and the appearance of a singlet at  $\delta = 24.0$  ppm (Figure S12) corresponding to a palladium bound  $\text{FcPPh}_2$ .<sup>[44]</sup>

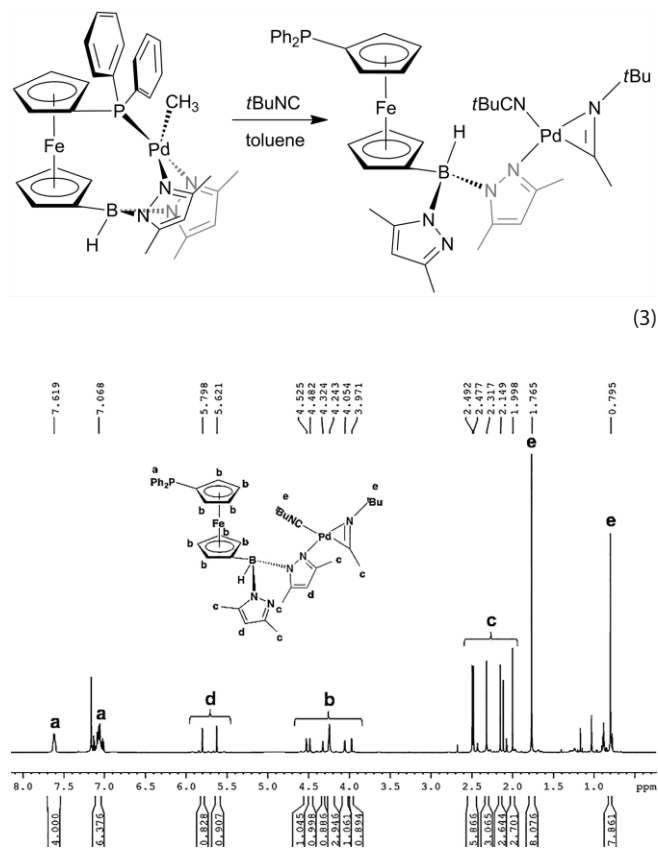


Figure 3.  $^1\text{H}$  NMR spectrum ( $\text{C}_6\text{D}_6$ , 500 MHz, 298 K) of  $(\text{fc}^{\text{PB}})\text{Pd}[\text{C}(\text{Me})\text{NtBu}](\text{CNtBu})$ .

### Polymerization of Norbornene and Norbornene Derivatives

The reduced ferrocene complex,  $(\text{fc}^{\text{PB}})\text{PdMe}$ , in the presence of norbornene showed no polymerization activity even when heating up to  $100\text{ }^\circ\text{C}$  in benzene. This absence of activity suggests that norbornene is too weak of a nucleophile to compete for a coordination site with the supporting ligand. On the other hand, in the presence of a stronger nucleophile, such as *tert*-butyl isocyanide, the phosphine of the supporting ligand is almost entirely displaced. Reducing the nucleophilic character of the supporting ligand through the oxidation of the ferrocene moiety, as was observed in the case of ferrocenyldiphenylphosphine coordination, promotes monomer coordination.

The oxidation of the ferrocene backbone with  $[\text{AcFc}][\text{BAR}^{\text{F}}]$  turns “on” the activity of the  $(\text{fc}^{\text{PB}})\text{PdMe}$  complex toward the polymerization of norbornene. The polymerization of 100 equiv. of norbornene (NB) reaches completion within an hour at  $70\text{ }^\circ\text{C}$ . However, the poor solubility of norbornene homopolymers in common organic solvents prevents their characterization by gel permeation chromatography (GPC) on regular instruments and complicates the in situ investigation of the “on/off” redox switch. To overcome these complications, norbornene derivatives (Figure 4) 5-butylbicyclo[2.2.1]hept-2-ene (NBa), 5-(triethoxysilyl)bicyclo[2.2.1]hept-2-ene (NBb), 5-(trimethylsilyl)bicyclo[2.2.1]hept-2-ene (NBc), and 5-cyclohexylbicyclo[2.2.1]hept-2-ene (NBd) were prepared and their polymerization results are summarized in Table 1. The polymerization of ca. 100 equiv. of the substituted norbornenes was monitored by  $^1\text{H}$  NMR spectroscopy, until no further monomer conversion was observed. The obtained polymers were characterized by gel permeation chromatography (GPC). A large discrepancy was found between the experimental and theoretical values of the molecular weights, suggesting a poorly controlled polymerization process, with the PDI ( $\text{PDI} = M_w/M_n$ ) values ranging from 1.5–3.6. A similar wide distribution of PDI values is observed in the literature for the polymerization of norbornenes by group 10 metals.<sup>[1,6,11,13,14,25]</sup> The polymerization activity for palladium complexes toward norbornene is largely dependent on the coordination environment around the metal center and the substituents on the monomer and can vary greatly from just a few numbers to several millions.<sup>[16,18,24,45]</sup> By comparison, the oxidized ferrocene heteroscorpionate complex shows a relatively low activity with turnover frequencies ranging from 12.5 to  $81\text{ mol}_{\text{nb}}\text{ mol}_{\text{Pd}}^{-1}\text{ h}^{-1}$ .

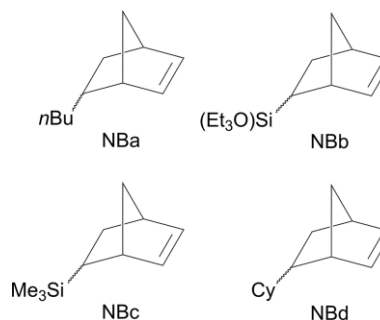


Figure 4. Norbornene derivatives NBa-d.

The in situ redox switch was performed with 5-triethoxysilyl norbornene. Starting with the oxidized complex  $[(\text{fc}^{\text{PB}})\text{PdMe}][\text{BAR}^{\text{F}}]$  in the presence of 100 equiv. of monomer results in the polymerization of 35 equiv. in 20 min at  $70\text{ }^\circ\text{C}$  (Table 1, entry 6). The addition of one equivalent of  $\text{Cp}_2\text{Co}$  relative to the palladium complex severely reduces the catalytic activity. The polymerization of 5 equiv. of NBb observed during this time can be attributed to a small number of catalytically active complex present in solution, due to the slow rate of reduction of the palladium compound by  $\text{Cp}_2\text{Co}$ , which takes up to 30 min at ambient temperature to reach completion. No further conversion upon heating of the reaction solution at  $70\text{ }^\circ\text{C}$  for 20 min is observed once the reduction process is complete.

Table 1. Polymerization of norbornene derivatives by in situ generated  $[(\text{fc}^{\text{Pb}})\text{PdMe}][\text{BAR}^{\text{F}}]$ .<sup>[a]</sup>

| Entry | Monomer | Time [h] | Conv. [%] | $M_n$ theo | $M_n$ exp | PDI  | TOF  |
|-------|---------|----------|-----------|------------|-----------|------|------|
| 1     | NB      | 1        | 78        | –          | –         | –    | 64   |
| 2     | NBa     | 1        | 79        | 12.2       | 30.6      | 3.63 | 81   |
| 3     | NBb     | 1        | 58        | 14.9       | 37.0      | 2.52 | 58   |
| 4     | NBc     | 0.5      | 33        | 5.8        | 8.8       | 2.10 | 70   |
| 5     | NBd     | 2        | 27        | 4.4        | 1.4       | 1.46 | 12.5 |
| 6     | NBb     | 1.33     | 49        | 13.0       | 30.5      | 3.04 | 38.3 |

[a] Conditions: Monomer (0.50 mmol), catalyst (0.005 mmol), oxidant (0.005 mmol),  $[\text{D}_6]$ benzene as a solvent (0.5 mL) and 1,3,5-trimethoxybenzene (0.10 mmol) as an internal standard. All experiments were performed at 70 °C, except for entry 5, performed at 100 °C.  $M_n$  are reported in  $10^3$  g/mol; PDI =  $M_w/M_n$ , TOF =  $(\text{mol}_{\text{NB}} \text{ in polymer}) \text{ mol}_{\text{Pd}}^{-1} \text{ h}^{-1}$ . In the case of entry 1, the isolated yield is reported instead of conversion.

The oxidation with  $[\text{AcFc}][\text{BAR}^{\text{F}}]$  restores the catalytic activity (Figure 5). The slow rate of reduction of the catalyst would account for the shoulder peak observed in the GPC graph of the isolated polymer (Figure S37).

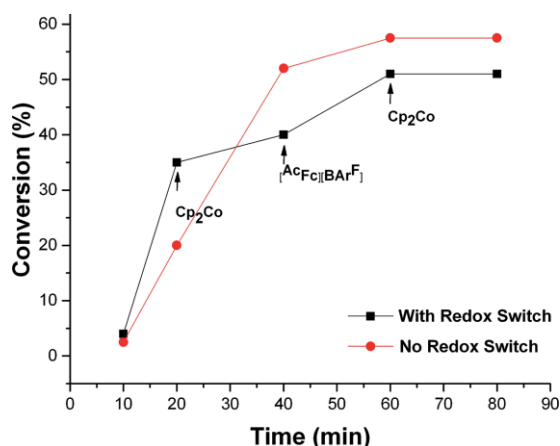


Figure 5. Comparison of 5-(triethoxysilyl)-bicyclo[2.2.1]hept-2-ene polymerization using a redox switch and not using a redox switch using  $[(\text{fc}^{\text{Pb}})\text{PdMe}][\text{BAR}^{\text{F}}]$  as a catalyst.

To gain a better understanding of how the redox switches affect the polymerization reaction, the influence of ligand oxidation upon electron-donating abilities of individual ferrocene substituents was considered. The oxidation of ferrocenyldiphenylphosphine reduces the electron-donating ability of the phosphine donor, resulting in the increase of the CO stretching frequency by several wave numbers in rhenium carbonyl complexes.<sup>[46]</sup> Alternatively, oxidation of a ferrocene containing tris(pyrazolyl)borate carbonylmolybdenum complex resulted in virtually no change in the stretching frequency of the carbonyl ligands.<sup>[47]</sup> Based on these literature reports and our experimental results, we propose that the oxidation of the ferrocene-chelating heteroscorpionate increases the lability of the phosphine moiety allowing monomer coordination and migratory insertion into the alkyl–metal fragment, while the (pyrazolyl)-borate portion remains unaffected. Since the displacement of the phosphine in the reduced complex by norbornene does not occur, the polymerization process is halted with this catalyst.

The involvement of alternative mechanisms in the polymerization of norbornene was also considered. In principle, “naked”  $\text{Pd}^{2+}$  might be generated in situ through loss of the supporting ligands; such species yield high molecular weight polynorbornenes.<sup>[48]</sup> However, the influence of the redox switch on the polymerization of norbornene suggests that the supporting ligand remains attached to palladium throughout the polymerization process. Alternatively, polymerization of norbornene by a cationic mechanism yields oligomeric materials with low molecular weights.<sup>[49]</sup> The reaction of norbornenes with  $[\text{AcFc}][\text{BAR}^{\text{F}}]$  (Figure S25–S28) under similar polymerization conditions as those used for  $[(\text{fc}^{\text{Pb}})\text{PdMe}][\text{BAR}^{\text{F}}]$  yielded no isolable polymeric material, suggesting that cationic polymerization by the oxidant is not a viable mechanism in this system.

## Conclusions

The application of a ferrocene-chelating heteroscorpionate ligand in palladium-catalyzed norbornene polymerization was investigated. Compound  $[(\text{fc}^{\text{Pb}})\text{PdMe}][\text{BAR}^{\text{F}}]$  shows a reversible on/off switch toward the polymerization of norbornene derivatives. While the reduced state of the catalyst,  $(\text{fc}^{\text{Pb}})\text{PdMe}$ , shows no activity, the oxidized complex,  $[(\text{fc}^{\text{Pb}})\text{PdMe}][\text{BAR}^{\text{F}}]$ , exhibits activity toward norbornene polymerization.

## Experimental Section

**General Considerations:** All reactions were performed using standard Schlenk techniques or in an MBraun drybox (< 1 ppm  $\text{O}_2/\text{H}_2\text{O}$ ) unless noted otherwise. All glassware, cannulae, and Celite were stored in an oven at > 425 K before being brought into the drybox. Solvents were purified using a two-column solid-state purification system by the method of Grubbs<sup>[50]</sup> and transferred to the glovebox without exposure to air. NMR solvents were obtained from Cambridge Isotope Laboratories, degassed, and stored over activated molecular sieves prior to use. NMR spectra were recorded at ambient temperature on Bruker AV-300, AV-400, AV-500, and DRX-500 spectrometers unless otherwise noted. Proton and carbon chemical shifts are given relative to residual solvent peaks. Phosphorus, boron, and fluorine chemical shifts are given relative to external standards,  $\text{H}_3\text{PO}_4$ ,  $\text{Et}_2\text{O}\cdot\text{BF}_3$ , and trifluoroacetic acid, respectively.  $(\text{fc}^{\text{Pb}})\text{Li}(\text{THF})_2$ <sup>[38]</sup> was prepared using a literature procedure, and, unless otherwise noted, all reagents were acquired from commercial sources and used as received. Elemental analyses were performed on an Exeter Analytical, Inc. CE-440 Elemental Analyzer. Molecular weights of the polymers were determined by GPC-LLS (Gel Permeation Chromatography, Laser Light Scattering). GPC-LLS uses an Agilent liquid chromatograph equipped with an Agilent 1200 series pump and autosampler, three Phenogel 5  $\mu\text{m}$  Narrow Bore columns, a Wyatt Optilab differential refractometer, Wyatt Tristar miniDAWN and a Wyatt Viscostar viscometer. A flow rate of 1.0 mL/min was used and samples were dissolved in chloroform with 0.25 % triethylamine. Results were calibrated to narrow molecular weight polystyrene standards.

**(COD)PdMeCl:** A suspension of (COD)PdCl<sub>2</sub> (247.7 mg, 0.868 mmol) in 6 mL of Et<sub>2</sub>O/THF (1:2 vol %) was cooled to –78 °C. Trimethylaluminum (125.1 mg, 1.735 mmol) in 1 mL of hexanes was added slowly, the reaction mixture was removed from the cold well, and stirred at ambient temperature until the solution became colorless.

Methanol was added to solvolyze the aluminum by-products and volatile substances were removed under reduced pressure. The desired product was extracted with THF and filtered through Celite. THF was removed under reduced pressure and the resulting off-white solids were washed with Et<sub>2</sub>O (2 × 2 mL) to afford the final product (185.3 mg, 80.5 %). This procedure was carried out multiple times in similar scales with yields ranging from 50–80 %. <sup>1</sup>H NMR (CDCl<sub>3</sub>, 500 MHz, 298 K): δ = 1.18 (s, 3 H, PdCH<sub>3</sub>), 2.47 (m, 4 H, CH<sub>2</sub>), 2.58 (m, 2 H, CH<sub>2</sub>), 2.65 (m, 2 H, CH<sub>2</sub>), 5.15 (t, 2 H, CH), 5.91 (t, 2 H, CH) ppm.

**(f<sup>c</sup>P<sup>B</sup>)PdMe:** To (COD)PdMeCl (155.1 mg, 0.585 mmol) in 10 mL of THF, (f<sup>c</sup>P<sup>B</sup>)Li(THF)<sub>2</sub> (384.3 mg, 0.532 mmol) in 5 mL of THF was added dropwise. The reaction solution was stirred for 16 h at ambient temperature. Volatile substances were removed under reduced pressure and the desired product was extracted into 10 mL of toluene and filtered through Celite. Reduction in volume of the toluene solution to 4 mL and layering with 4 mL of hexanes afforded red crystalline material after 24 h at –35 °C. Decanting of the solution and washing of the remaining solids with hexanes (3 × 2 mL) and cold toluene (3 × 1 mL) yields the product as a red crystalline material (321.9 mg, 77.1 %) in two crops. Crystals of (f<sup>c</sup>P<sup>B</sup>)PdMe always contain one molecule of toluene per molecule of compound as supported by NMR spectroscopic data. X-ray quality crystals were obtained from toluene at –35 °C. <sup>1</sup>H NMR (C<sub>6</sub>D<sub>6</sub>, 500 MHz, 298 K): δ = 0.99 (d, 3 H, PdCH<sub>3</sub>), 1.65 (s, 3 H, CCH<sub>3</sub>), 2.30 (s, 3 H, CCH<sub>3</sub>), 2.35 (s, 3 H, CCH<sub>3</sub>), 2.42 (s, 3 H, CCH<sub>3</sub>), 3.18 (s, 1 H, Cp-H), 3.95 (s, 1 H, Cp-H), 4.04 (s, 1 H, Cp-H), 4.18 (s, 1 H, Cp-H), 4.21 (s, 1 H, Cp-H), 4.30 (s, 1 H, Cp-H), 4.43 (s, 1 H, Cp-H), 5.04 (s, 1 H, Cp-H), 5.56 (s, 1 H, CH), 5.73 (s, 1 H, CH), 6.92 (t, 2 H, p-Ph), 7.05 (m, 4 H, m-Ph), 7.41 (t, 2 H, o-Ph), 7.57 (t, 2 H, o-Ph) ppm. <sup>13</sup>C NMR (C<sub>6</sub>D<sub>6</sub>, 126 MHz, 298 K): δ = –0.98 (d, PdCH<sub>3</sub>), 14.2 (s, CCH<sub>3</sub>), 14.3 (d, CCH<sub>3</sub>), 14.4 (s, CCH<sub>3</sub>), 15.3 (s, CCH<sub>3</sub>), 68.9 (s, Cp-C), 69.5 (s, Cp-C), 70.8 (d, Cp-C), 72.4 (d, Cp-C), 73.8 (d, Cp-C), 74.7 (s, Cp-C), 74.9 (d, Cp-C), 80.2 (s, Cp-C), 105.8 (s, -CH-), 106.7 (d, -CH-), 132.2 (s, aromatic), 132.6 (s, aromatic), 133.6 (s, aromatic), 133.7 (s, aromatic), 133.9 (s, aromatic), 134.0 (s, aromatic), 134.1 (s, aromatic), 134.2 (s, aromatic), 145.4 (s, CCH<sub>3</sub>), 146.4 (d, CCH<sub>3</sub>), 147.9 (s, CCH<sub>3</sub>), 148.8 (d, CCH<sub>3</sub>) ppm. <sup>11</sup>B NMR (C<sub>6</sub>D<sub>6</sub>, 161 MHz, 298 K): δ = –7.6 (br. s) ppm. <sup>31</sup>P[<sup>1</sup>H] NMR (C<sub>6</sub>D<sub>6</sub>, 121 MHz, 298 K): δ = 30.5 (s) ppm. Anal. Calcd: (f<sup>c</sup>P<sup>B</sup>)PdMe·(C<sub>7</sub>H<sub>8</sub>) (C<sub>40</sub>H<sub>44</sub>BF<sub>2</sub>Fe<sub>4</sub>PPd) C, 61.21; H, 5.65; N, 7.14; found C, 60.82; H, 5.00; N, 6.56.

**[(f<sup>c</sup>P<sup>B</sup>)PdMe][BAR<sup>F</sup>]:** To [f<sup>c</sup>Fc][BAR<sup>F</sup>] (75.9 mg, 0.069 mmol) was added (f<sup>c</sup>P<sup>B</sup>)PdMe·(C<sub>7</sub>H<sub>8</sub>) (49.6 mg, 0.063 mmol) in 5 mL of toluene. The reaction solution was stirred for 10 min and filtered through Celite. The solution volume was reduced to 1 mL, diluted to 10 mL with hexanes, and stored at –35 °C for 30 min. Decanting of the solution and washing of the remaining brown oil with cold hexanes (2 × 4 mL) yields the product as a brown solid after an hour under reduced pressure (84.3 mg, 81.2 %). <sup>1</sup>H NMR (C<sub>6</sub>D<sub>6</sub>, 500 MHz, 298 K): δ = –9.71 (br. s), –3.28 (s), –1.82 (s), 1.68 (s), 3.58 (br. s), 4.68 (s), 4.84 (s), 7.42 (s), 7.91 (s), 8.60 (s), 10.04 (s), 12.43 (br. s) ppm. <sup>11</sup>B NMR (C<sub>6</sub>D<sub>6</sub>, 161 MHz, 298 K): δ = –65.2 (br. s), –6.1 (s) ppm. <sup>19</sup>F NMR (C<sub>6</sub>D<sub>6</sub>, 282 MHz, 298 K): δ = –62.2 (s) ppm. Anal. Calcd: [(f<sup>c</sup>P<sup>B</sup>)PdMe][BAR<sup>F</sup>]·(C<sub>7</sub>H<sub>8</sub>) (C<sub>72</sub>H<sub>56</sub>B<sub>2</sub>F<sub>24</sub>Fe<sub>4</sub>PPd) C, 52.47; H, 3.43; N, 3.40; found C, 51.97; H, 2.74; N, 3.25.

**(f<sup>c</sup>P<sup>B</sup>)Pd[C(Me)NtBu](CNtBu):** To (f<sup>c</sup>P<sup>B</sup>)PdMe·(C<sub>7</sub>H<sub>8</sub>) (113.3 mg, 0.144 mmol) in 5 mL of dichloromethane at –78 °C was added CNtBu (0.065 mL, 0.577 mmol) via syringe. The reaction mixture was stirred for 1 h at –78 °C before volatile substances were removed under reduced pressure. The desired product was extracted in 3 mL of diethyl ether and filtered through Celite. Diethyl ether was removed under reduced pressure and the remaining solids were dis-

solved in 1.5 mL of toluene containing 2 drops of tBuNC. Hexanes (1 mL) was layered on top and the solution was stored overnight at –35 °C. Decanting of the solution and washing of the remaining solids with hexanes (3 × 1 mL) yielded the final product as an orange crystalline material (97.5 mg, 71.2 %). Crystals of (f<sup>c</sup>P<sup>B</sup>)Pd[C(Me)NtBu](CNtBu) always contain one molecule of toluene per molecule of compound as supported by NMR spectroscopic data. <sup>1</sup>H NMR (C<sub>6</sub>D<sub>6</sub>, 500 MHz, 298 K): δ = 0.79 [s, 9 H, C(CH<sub>3</sub>)<sub>3</sub>], 1.76 [s, 9 H, C(CH<sub>3</sub>)<sub>3</sub>], 2.00 (s, 3 H, CH<sub>3</sub>), 2.15 (s, 3 H, CH<sub>3</sub>), 2.32 (s, 3 H, CH<sub>3</sub>), 2.48 (s, 3 H, CH<sub>3</sub>), 2.49 (s, 3 H, CH<sub>3</sub>), 3.97 (m, 1 H, Cp-H), 4.05 (m, 1 H, Cp-H), 4.24 (m, 3 H, Cp-H), 4.32 (m, 1 H, Cp-H), 4.48 (m, 1 H, Cp-H), 4.52 (m, 1 H, Cp-H), 5.62 (s, 1 H, CH), 5.80 (s, 1 H, CH), 7.07 (m, 6 H, m-Ph, p-Ph), 7.62 (m, 4 H, o-Ph) ppm. <sup>13</sup>C NMR (C<sub>6</sub>D<sub>6</sub>, 126 MHz, 298 K): δ = 13.7 (s, CCH<sub>3</sub>), 14.8 (s, CCH<sub>3</sub>), 15.0 (s, CCH<sub>3</sub>), 15.8 (s, CCH<sub>3</sub>), 29.7 [s, C(CH<sub>3</sub>)<sub>3</sub>], 32.2 [s, C(CH<sub>3</sub>)<sub>3</sub>], 34.4 [s, C(CH<sub>3</sub>)=NC(CH<sub>3</sub>)<sub>3</sub>], 56.5 [s, C(CH<sub>3</sub>)<sub>3</sub>], 68.7 [s, C(CH<sub>3</sub>)=NC(CH<sub>3</sub>)<sub>3</sub>], 71.0 (s, Cp-C), 72.7 (d, Cp-C), 73.0 (d, Cp-C), 73.6 (s, Cp-C), 73.8 (s, Cp-C), 74.8 (s, Cp-C), 74.9 (s, Cp-C), 75.3 (s, Cp-C), 75.6 (s, Cp-C), 105.3 (s, CH), 106.5 (s, CH), 134.3 (s, aromatic), 134.4 (s, aromatic), 134.5 (s, aromatic), 134.6 (s, aromatic), 145.0 (s, CCH<sub>3</sub>), 145.4 (s, CCH<sub>3</sub>), 147.0 (s, CCH<sub>3</sub>), 149.1 (s, CCH<sub>3</sub>), 166.4 [C(CH<sub>3</sub>)=NC(CH<sub>3</sub>)<sub>3</sub>] ppm. <sup>11</sup>B NMR (C<sub>6</sub>D<sub>6</sub>, 161 MHz, 298 K): δ = 7.2 (br. s) ppm. <sup>31</sup>P[<sup>1</sup>H] NMR (C<sub>6</sub>D<sub>6</sub>, 121 MHz, 298 K): δ = –14.9 (s), 9.4 (s) ppm. Anal. Calcd: (f<sup>c</sup>P<sup>B</sup>)Pd[C(Me)NtBu](CNtBu)·(C<sub>7</sub>H<sub>8</sub>) (C<sub>50</sub>H<sub>62</sub>BF<sub>2</sub>Fe<sub>4</sub>PPd) C, 63.14; H, 6.57; N, 8.84; found C, 62.62; H, 6.49; N, 8.86.

**General Procedure for Synthesis of Substituted Norbornenes:** A pressure reactor was charged with dicyclopentadiene (20.0 mmol) and the corresponding olefin (44.0 mmol). The reactor was purged with nitrogen and sealed. The reactor was then heated to 220–240 °C for two hours before being cooled to ambient temperature. The reactor was opened and the resulting tan oil was distilled at 2.5 Torr to afford a colorless liquid.

**5-Butylbicyclo[2.2.1]hept-2-ene (NBa):** Distilled at 35 °C and 2.5 Torr to afford a colorless liquid (44.0 %), 18.2 % *exo*, 81.8 % *endo*. <sup>1</sup>H NMR (CDCl<sub>3</sub>, 500 MHz, 298 K): δ = 0.47–0.50 (m, 1 H), 0.87 (m, 3 H), 1.07 (m, 2 H), 1.20–1.46 (m, 6 H), 1.82 (m, 1 H), 1.96 (m, 1 H), 2.50 (s, 1 H), 2.75 (s, 1 H), 5.54–6.11 (m, 2 H, olefinic) ppm. <sup>13</sup>C NMR (CDCl<sub>3</sub>, 500 MHz, 298 K): δ = 137.1, 137.0, 136.3, 133.4, 132.6, 132.5, 54.4, 49.7, 48.3, 46.5, 45.8, 45.6, 45.4, 42.7, 42.1, 41.6, 38.9, 36.9, 36.5, 34.7, 33.2, 32.6, 31.3, 31.1, 23.1, 14.2 ppm.

**5-(Triethoxysilyl)bicyclo[2.2.1]hept-2-ene (NBb):** Distilled at 65 °C and 2.5 Torr to afford a colorless liquid (46.8 %) as a mixture of *exo* and *endo* isomers. <sup>1</sup>H NMR (CDCl<sub>3</sub>, 500 MHz, 298 K): δ = 0.46 (m, 1 H), 1.07 (m, 1 H), 1.23 (m, 9 H), 1.35 (m, 1 H), 1.76 (m, 1 H), 1.88 (m, 1 H), 2.92 (m, 2 H), 3.76–3.86 (m, 6 H), 5.92–6.13 (m, 2 H, olefinic) ppm. <sup>13</sup>C NMR (CDCl<sub>3</sub>, 500 MHz, 298 K): δ = 137.9, 135.4, 134.8, 133.8, 58.6, 58.4, 47.1, 44.3, 42.9, 42.6, 42.3, 27.1, 26.4, 20.9, 20.4, 18.5, 18.4 ppm.

**5-(Trimethylsilyl)bicyclo[2.2.1]hept-2-ene (NBc):** Distilled at 30 °C and 2.5 Torr to afford a colorless liquid (37.7 %) as a mixture of *exo* and *endo* isomers. <sup>1</sup>H NMR (CDCl<sub>3</sub>, 500 MHz, 298 K): δ = –0.09–0.00 (s, 9 H), 0.31 (m, 1 H), 0.90–1.14 (m, 2 H), 1.29–1.51 (m, 2 H), 1.85 (m, 1 H), 2.72–2.93 (m, 1 H), 3.21 (m, 1 H), 5.48–6.16 (m, 2 H, olefinic) ppm. <sup>13</sup>C NMR (CDCl<sub>3</sub>, 500 MHz, 298 K): δ = 138.7, 135.6, 134.1, 51.7, 47.0, 44.9, 43.0, 42.62, 42.57, 27.3, 27.1, 25.4, 25.3, –1.3, –1.8 ppm.

**5-Cyclohexylbicyclo[2.2.1]hept-2-ene (NBd):** Distilled at 76 °C at 2.5 Torr to afford a colorless liquid (7.53 %) <sup>1</sup>H NMR (CDCl<sub>3</sub>, 500 MHz, 298 K): δ = 0.60 (m, 2 H), 0.83–1.00 (m, 2 H), 1.12–1.20 (m, 4 H), 1.26 (s, 1 H), 1.36 (m, 1 H), 1.65 (m, 4 H), 1.77 (m, 2 H),

2.74–2.87 (s, 2 H), 5.90–6.10 (m, 2 H, olefinic) ppm.  $^{13}\text{C}$  NMR ( $\text{CDCl}_3$ , 500 MHz, 298 K):  $\delta = 137.1, 136.5, 132.4, 49.4, 46.0, 45.8, 45.5, 44.0, 43.1, 43.0, 42.5, 42.4, 41.9, 33.0, 32.8, 32.6, 32.5, 31.6, 31.2, 26.95, 29.93, 26.7, 26.6, 26.5, 26.4$  ppm.

**NMR Scale Polymerizations:** In a small vial,  $(\text{fc}^{\text{PB}})\text{PdMe}$  (5  $\mu\text{mol}$ ) was added to one equivalent of  $[\text{Fc}^{\text{C}}][\text{BAR}^{\text{F}}]$  in 0.2 mL of  $\text{C}_6\text{D}_6$  and stirred until the oxidant was consumed. To the oxidized complex was added an external standard, 1,3,5-trimethoxybenzene (0.1 mmol), and monomer (0.5 mmol); the total solution volume was increased to 0.5 mL of  $\text{C}_6\text{D}_6$ . The contents of the vial were stirred and the homogeneous solution was transferred to a J. Young NMR tube equipped with a Teflon valve. The NMR tube was sealed, taken out of the box and placed in an oil bath. The polymerization was monitored by  $^1\text{H}$  NMR spectroscopy until the conversion has stopped or reached completion. The contents of the NMR tube was diluted with 1 mL of dichloromethane and poured into 10 mL of methanol to yield white solids. The product was collected on a glass frit, washed with additional 5 mL of methanol and kept under reduced pressure until it reached a consistent weight. For the control experiments,  $[\text{Fc}^{\text{C}}][\text{BAR}^{\text{F}}]$  or  $\text{Cp}_2\text{Co}$  (5  $\mu\text{mol}$ ) was used instead of  $(\text{fc}^{\text{PB}})\text{PdMe}$  while the rest of the conditions above were kept the same.

**Electrochemical Studies:** Cyclic voltammetry studies were carried out in a 20 mL scintillation vial with electrodes fixed in position by a rubber stopper, in a 0.10 M tetrabutylammonium hexafluorophosphate solution in THF. A glassy carbon working electrode (planar circular area  $a = 0.071 \text{ cm}^2$ ), a platinum reference electrode (planar circular area:  $0.031 \text{ cm}^2$ ), and a silver-wire pseudo-reference electrode were purchased from CH Instruments. Before each cyclic voltammogram was recorded, the working and auxiliary electrodes were polished with an aqueous suspension of 0.05  $\mu\text{m}$  alumina on a microcloth polishing pad. Cyclic voltammograms were acquired with a CH Instruments CHI630D potentiostat and recorded with CH Instruments software (version 13.04) with data processing on Origin 9.2. All potentials are given with respect to the ferrocene/ferrocenium couple.

**X-ray Crystallography:** X-ray quality crystals were obtained from various concentrated solutions placed in a  $-35 \text{ }^\circ\text{C}$  freezer in the glove box unless otherwise specified. Inside the glove box, the crystals were coated with oil (STP Oil Treatment) on a microscope slide, which was brought outside the glove box. The X-ray data collections were carried out on a Bruker SMART 1000 single-crystal X-ray diffractometer using  $\text{Mo-K}_\alpha$  radiation and a SMART APEX CCD detector. The data was reduced by SAINTPLUS and an empirical absorption correction was applied using the package SADABS. The structure was solved and refined using SHELXTL (Bruker 1998, SMART, SAINT, XPRED AND SHELXTL, Bruker AXS Inc., Madison, Wisconsin, USA). Tables with atomic coordinates and equivalent isotropic displacement parameters, with all the bond lengths and angles, and with anisotropic displacement parameters are listed in the cif. CCDC 1452861 [for  $(\text{fc}^{\text{PB}})\text{PdMe}$ ] contains the supplementary crystallographic data for this paper. These data can be obtained free of charge from The Cambridge Crystallographic Data Centre.

## Acknowledgments

This work was supported by US National Science Foundation (NSF) (grant numbers 1362999, grant to P. L. D., and CHE-1048804) for NMR spectroscopy. The authors thank Mr. Jonathan Brosmer for assistance with elemental analysis experiments.

**Keywords:** Homogeneous catalysis · Polymerization · Palladium · Scorpionate ligands · Redox chemistry

- X. He, Y. Liu, L. Chen, Y. Chen, D. Chen, *J. Polym. Sci., Part A Polym. Chem.* **2012**, *50*, 4695–4704.
- C. Janiak, P. G. Lassahn, *J. Mol. Catal. A* **2001**, *166*, 193–209.
- S. Ahmed, S. A. Bidstrup, P. A. Kohl, P. J. Ludovice, *J. Phys. Chem. B* **1998**, *102*, 9783–9790.
- N. R. Grove, P. A. Kohl, S. A. Bidstrup Allen, S. Jayaraman, R. Shick, *J. Polym. Sci., Part B: Polym. Phys.* **1999**, *37*, 3003–3010.
- B. S. Heinz, F. P. Alt, W. Heitz, *Macromol. Rapid Commun.* **1998**, *19*, 251–256.
- T. F. A. Haselwander, W. Heitz, S. A. Krügel, J. H. Wendorff, *Macromol. Chem. Phys.* **1996**, *197*, 3435–3453.
- F. Blank, C. Janiak, *Coord. Chem. Rev.* **2009**, *253*, 827.
- Q. Wu, Y. Lu, *J. Polym. Sci., Part A: Polym. Chem.* **2002**, *40*, 1421–1425.
- P. Huo, W. Liu, X. He, Z. Wei, Y. Chen, *Polym. Chem.* **2014**, *5*, 1210–1218.
- F. Blank, J. K. Vieth, J. Ruiz, V. Rodríguez, C. Janiak, *J. Organomet. Chem.* **2011**, *696*, 473–487.
- E. J. Lee, W. K. Won, B. Lee, Y. H. Kye, I. M. Lee, *Bull. Korean Chem. Soc.* **2013**, *34*, 2720–2724.
- M. Kang, A. Sen, *Organometallics* **2004**, *23*, 5396–5398.
- T. Hu, Y.-G. Li, Y.-S. Li, N.-H. Hu, *J. Mol. Catal. A* **2006**, *253*, 155–164.
- J. Tian, H. Zhu, J. Liu, D. Chen, X. He, *Appl. Organomet. Chem.* **2014**, *28*, 702–711.
- A. D. Hennis, J. D. Polley, G. S. Long, A. Sen, D. Yandulov, J. Lipian, G. M. Benedikt, L. F. Rhodes, J. Huffman, *Organometallics* **2001**, *20*, 2802–2812.
- M. D. Walter, R. A. Moorhouse, S. A. Urbin, P. S. White, M. Brookhart, *J. Am. Chem. Soc.* **2009**, *131*, 9055–9069.
- J. A. Casares, P. Espinet, G. Salas, *Organometallics* **2008**, *27*, 3761–3769.
- M. Yamashita, I. Takamiya, K. Jin, K. Nozaki, *Organometallics* **2006**, *25*, 4588–4595.
- F. Blank, H. Scherer, C. Janiak, *J. Mol. Catal. A* **2010**, *330*, 1–9.
- F. Blank, H. Scherer, J. Ruiz, V. Rodríguez, C. Janiak, *Dalton Trans.* **2010**, *39*, 3609–3619.
- C. Mehler, W. Risse, *Macromolecules* **1992**, *25*, 4226–4228.
- C. Mehler, W. Risse, *Makromol. Chem. Rapid Commun.* **1991**, *12*, 255–259.
- B. S. Heinz, W. Heitz, S. A. Krügel, F. Raubacher, J. H. Wendorff, *Acta Polym.* **1997**, *48*, 385–391.
- D.-G. Kim, A. Bell, R. A. Register, *ACS Macro Lett.* **2015**, *4*, 327–330.
- P. Xiang, Z. Ye, *J. Organomet. Chem.* **2015**, *798*, Part 2, 429–436.
- F. Blank, C. Janiak, *Coord. Chem. Rev.* **2009**, *253*, 827–861.
- B. Commarieu, J. P. Claverie, *Chem. Sci.* **2015**, *6*, 2172–2181.
- S. Mecking, W. Keim, *Organometallics* **1996**, *15*, 2650–2656.
- A. M. Allgeier, C. A. Mirkin, *Angew. Chem. Int. Ed.* **1998**, *37*, 894–908; *Angew. Chem.* **1998**, *110*, 936.
- X. Wang, J. L. Brosmer, A. Thevenon, P. L. Diaconescu, *Organometallics* **2015**, *34*, 4700–4706.
- S. M. Quan, P. L. Diaconescu, *Chem. Commun.* **2015**, *51*, 9643–9646.
- X. Wang, A. Thevenon, J. L. Brosmer, I. Yu, S. I. Khan, P. Mehrkhodavandi, P. L. Diaconescu, *J. Am. Chem. Soc.* **2014**, *136*, 11264–11267.
- E. M. Broderick, N. Guo, T. Wu, C. S. Vogel, C. Xu, J. Sutter, J. T. Miller, K. Meyer, T. Cantat, P. L. Diaconescu, *Chem. Commun.* **2011**, *47*, 9897–9899.
- E. M. Broderick, N. Guo, C. S. Vogel, C. Xu, J. Sutter, J. T. Miller, K. Meyer, P. Mehrkhodavandi, P. L. Diaconescu, *J. Am. Chem. Soc.* **2011**, *133*, 9278–9281.
- F. T. Ladipo, G. K. Anderson, *Organometallics* **1994**, *13*, 303–306.
- E. V. Salo, Z. Guan, *Organometallics* **2003**, *22*, 5033–5046.
- L. Yang, D. R. Powell, R. P. Houser, *Dalton Trans.* **2007**, 955–964.
- M. Abubekerev, P. L. Diaconescu, *Inorg. Chem.* **2015**, *54*, 1778–1784.
- A. W. Waltman, R. H. Grubbs, *Organometallics* **2004**, *23*, 3105–3107.
- A. L. Rheingold, L. M. Liable-Sands, C. L. Incarvito, S. Trofimenko, *J. Chem. Soc., Dalton Trans.* **2002**, 2297–2301.
- J. G. P. Delis, P. G. Aubel, K. Vrieze, P. W. N. M. van Leeuwen, N. Veldman, A. L. Spek, F. J. R. van Neer, *Organometallics* **1997**, *16*, 2948–2957.
- J. G. P. Delis, P. G. Aubel, P. W. N. M. van Leeuwen, K. Vrieze, N. Veldman, A. L. Spek, *J. Chem. Soc., Chem. Commun.* **1995**, 2233–2234.
- Y. Yamamoto, T. Tanase, H. Ukaji, M. Hasegawa, T. Igoshi, K. Yoshimura, *J. Organomet. Chem.* **1995**, *498*, C23–C26.

- [44] S. Otto, *J. Chem. Crystallogr.* **2001**, *31*, 185–190.
- [45] A. D. Hennis, J. D. Polley, G. S. Long, A. Sen, D. Yandulov, J. Lipian, G. M. Benedikt, L. F. Rhodes, J. Huffman, *Organometallics* **2001**, *20*, 2802–2812.
- [46] T. M. Miller, K. J. Ahmed, M. S. Wrighton, *Inorg. Chem.* **1989**, *28*, 2347–2355.
- [47] F. Fabrizi de Biani, F. Jäkle, M. Spiegler, M. Wagner, P. Zanello, *Inorg. Chem.* **1997**, *36*, 2103–2111.
- [48] P.-G. Lassahn, V. Lozan, B. Wu, A. S. Weller, C. Janiak, *Dalton Trans.* **2003**, 4437–4450.
- [49] N. G. Gaylord, B. M. Mandal, M. Martan, *J. Polym. Sci. Polym. Lett. Ed.* **1976**, *14*, 555–559.
- [50] A. B. Pangborn, M. A. Giardello, R. H. Grubbs, R. K. Rosen, F. J. Timmers, *Organometallics* **1996**, *15*, 1518–1520.

---

Received: November 7, 2015

Published Online: February 12, 2016